FF

EUROPEAN ORGANIZATION FOR NUCLEAR RESEARCH
EUROPEAN LABORATORY FOR PARTICLE PHYSICS

CERN-TIS-99-020-RP-PP

NEUTRON MEASUREMENTS AROUND A BEAM DUMP BOMBARDED BY HIGH ENERGY PROTONS AND LEAD IONS

S. Agosteo[1,2], C. Birattari[2,3], A. Foglio Para[1], M. Silari[4], L. Ulrici[4].

(1) Dipartimento di Ingegneria Nucleare, Politecnico di Milano, via Ponzio 34/3, 20133 Milano, Italy.
(2) Istituto Nazionale di Fisica Nucleare, Sezione di Milano, via Celoria 16, 20133 Milano, Italy
(3) Università degli Studi di Milano, Dipartimento di Fisica, via Celoria 16, 20133 Milano, Italy.
(4) CERN, 1211 Geneva 23, Switzerland.

ABSTRACT

Measurements of the spectral fluence and the ambient dose equivalent of secondary neutrons produced by 250 GeV/c protons and 158 GeV/c per nucleon lead ions were performed at CERN around a thick beam dump. The experimental results obtained with protons were compared with calculations performed with the FLUKA Monte Carlo code. As the available Monte Carlo codes do not transport particles with mass larger than one atomic mass unit, it is shown that for high energy heavy ions estimates can be carried out by scaling the result of a Monte Carlo calculation for protons by the projectile mass number.

Submitted for publication in Nuclear Instruments and Methods A

CERN, Geneva, Switzerland
17 December 1999

1. Introduction

The transverse shielding of high energy proton accelerators mainly involves the attenuation of the secondary neutrons generated in the hadronic cascade. A first estimate can be obtained by the well-known two-parameter formula of the Moyer model [1, 2], which in case of a simple structure often provides sufficiently accurate results. To verify the preliminary analytical calculations or in case of a complex geometry, one has to resort to a detailed Monte Carlo calculation. However, for ions heavier than protons, most of the available Monte Carlo codes, such as FLUKA [3, 4], LAHET [5] and MARS [6], cannot be employed directly because they do not transport ions with mass larger than one atomic mass unit. The purpose of this paper is to show that for high energy heavy ions estimates can be carried out by scaling the result of a Monte Carlo calculation for protons by the projectile mass number, considering the ion projectile as a bunch of free protons.

Measurements of the stray neutron component produced by high energy protons and lead ions were performed at CERN around a thick beam dump. The dump was designed to absorb completely both protons (actually, a mixed beam of 2/3 protons and 1/3 positive pions) and lead ions accelerated to several hundreds GeV per nucleon. The measurements were performed on the top of the dump using different types of rem counters and a Bonner sphere spectrometer, with a primary beam of 250 GeV/c protons/pions and 158 GeV/c per nucleon lead ions. For the former case, Monte Carlo simulations were performed with the FLUKA code to evaluate the neutron spectral fluence and the ambient dose equivalent and the results compared with the experimental data. Preliminary results were reported in two conference proceedings [7, 8] and some of them are recalled in the following for the sake of completeness.

2. The beam dump

An interesting opportunity to make comparative measurements, outside a thick shield, of the secondary neutrons produced by high energy proton and lead ion beams was available in the North Experimental Area of CERN (on the Prevessin site of the Laboratory), where several experiments installed in four beam lines are provided with high-energy beams from the Super Proton Synchrotron (SPS). The present experiment was conducted around an iron/concrete dump separating two experimental areas in one of the beam lines. The measurements were performed with a 250 GeV/c proton beam slow extracted over 2.6 s within a repetition rate of 14.4 s, and with a $^{208}Pb^{82+}$ beam accelerated to 158 GeV/c per nucleon or 33 TeV total energy in pulses 4.8 s long with a repetition rate of 19.2 s. The measurements were carried out in April and October 1998, parasitically during physics data taking.

The dump was designed [7] for a limit intensity of 5×10^6 lead ions per SPS pulse accelerated to 158 GeV/c per nucleon. The structure consists of an iron core 3.2 m thick, surrounded and backed by 1.6 m concrete and with additional 1.6 m concrete in front with a 40 cm collimator opening. The latter was designed to trap backscattered particles and thus reduce the background in the upstream experimental area. The design specifications of the iron core required 160 cm in the transverse direction. The dump is made up of blocks of standard dimensions which are multiple of 40 cm. The iron core was in a first instance built without following correctly the specifications, i.e. by aligning on the beam axis blocks with the required total length of 3.2 m but with transverse dimensions of 160 cm (horizontal) x 80 cm (vertical). As this configuration only provided 40 cm iron in the vertical direction to the beam axis, additional 40 cm iron were added on top of the core. However, only the first 2.4 m of the core were then covered with the specified 1.6 m of concrete. The final shape of the dump is sketched in Fig. 1.

Monte Carlo simulations were performed with the FLUKA code for several primary proton momentum (namely 50, 100, 158, 250 and 400 GeV/c) both to check the analytical estimates and to calculate the neutron spectral fluence at various positions [7]. In a first step, the dump was modelled as a cylinder (a cylindrical iron core enclosed in a cylindrical concrete shell), because the axial

symmetry conserves the shielding thickness "seen" by the secondary particles produced along the primary beam track and escaping from the lateral surface. This permitted scoring into concentric cylindrical shells (i.e. rings) in contact with the lateral concrete surface in order to reduce the computing time. The results of the simulations were compared with measurements performed at 250 GeV/c at various positions on the top and in front of the dump. The simulated ambient dose equivalent was lower by a factor of 2 than that measured in most positions, suggesting that the cylindrical approximation might have some limitations. The simulated spectral fluences were used as a guess for adjusting the measured spectra in the unfolding procedure. The consistency of the simulated spectra with those measured was satisfactory. The real beam dump geometry was modelled in a further set of FLUKA simulations for a 250 GeV/c hadron beam, described in ref. [8] and briefly recalled in the following section.

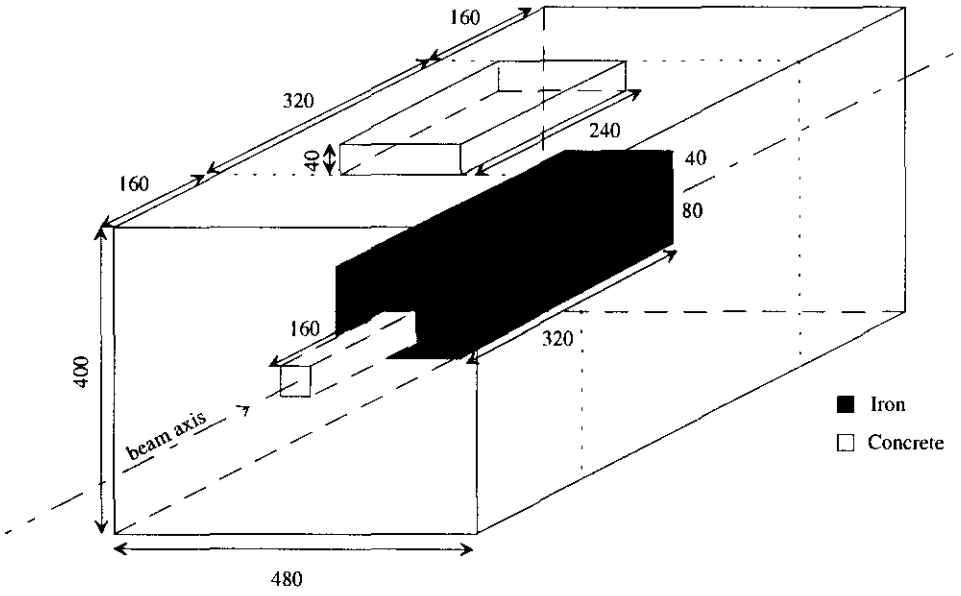

Fig. 1 A schematic view of the beam dump. Dimensions are in centimetres.

3. Simulations of the real dump geometry

The simulations of the real beam dump geometry were performed for a 250 GeV/c proton and positive pion beam, separately. It should be emphasised that modelling the "real" geometry is quite difficult in the present case. In fact, as mentioned in the previous section, the dump is assembled with concrete and iron modules of standard dimensions so that slits and openings in between adjacent blocks cannot be completely avoided. The depth and width of such openings cannot be accurately measured because of the large dimensions of the whole structure. The geometry simulated at first reproduced strictly that of the real structure, but neglecting all slits and openings. Geometry splitting and Russian Roulette were adopted as variance reduction techniques for neutrons by subdividing fictitiously the concrete layer into parallelepiped shells 20 cm thick. The neutron fluence was tracked in a grid of void parallelepiped cells (width 160 cm, length 80 cm, thickness 40 cm) on the top surface of the dump, thus reproducing the measurement positions sketched in Fig. 2. The resulting values of ambient dose equivalent, calculated at locations C2-C5 with the conversion coefficients of ref. [9], are listed in Table 1. The contribution of pure pion and proton beams is listed separately, together with that of the experimental beam (2/3 protons and 1/3 pions).

The influence of the incomplete geometry modelling was investigated in a further set of simulations, as the results obtained with the model described above were lower than the

Table 1. Neutron ambient dose equivalent on the top of the dump. The scoring is made on parallelepiped regions 80 cm wide laterally (see Fig. 2). The positions are labelled C2 to C5 for consistency with results reported previously [7, 8]. The values are normalised to primary particle impinging on the centre of the iron core. The basic geometry is shown in Fig. 1.

	Basic geometry (pions only)	Basic geometry (protons only)	Reduced scoring cell thickness only C3-C5 (protons only)	Plus lateral wall and air (protons only)	With opening between C2 and C3, no wall, no air (protons only)	Basic geometry (2/3 protons, 1/3 pions), Fig. 1	Measurements LINUS
Position	Ambient dose equivalent per primary particle (Sv)						
C2	$(2.10\pm0.03)\times10^{-16}$	$(2.70\pm0.06)\times10^{-16}$	-	$(2.61\pm0.11)\times10^{-16}$	$(3.53\pm0.21)\times10^{-16}$	$(2.50\pm0.05)\times10^{-16}$	-
C3	$(1.49\pm0.05)\times10^{-16}$	$(1.74\pm0.02)\times10^{-16}$	$(1.90\pm0.03)\times10^{-16}$	$(1.88\pm0.09)\times10^{-16}$	$(2.02\pm0.13)\times10^{-16}$	$(1.66\pm0.03)\times10^{-16}$	$(4.74\pm0.59)\times10^{-16}$
C4	$(1.92\pm0.03)\times10^{-16}$	$(2.24\pm0.03)\times10^{-16}$	$(2.48\pm0.04)\times10^{-16}$	$(2.49\pm0.08)\times10^{-16}$	$(2.28\pm0.18)\times10^{-16}$	$(2.13\pm0.03)\times10^{-16}$	$(4.16\pm0.53)\times10^{-16}$
C5	$(1.44\pm0.06)\times10^{-16}$	$(1.57\pm0.02)\times10^{-16}$	$(1.71\pm0.03)\times10^{-16}$	$(1.69\pm0.08)\times10^{-16}$	$(1.60\pm0.16)\times10^{-16}$	$(1.53\pm0.04)\times10^{-16}$	-

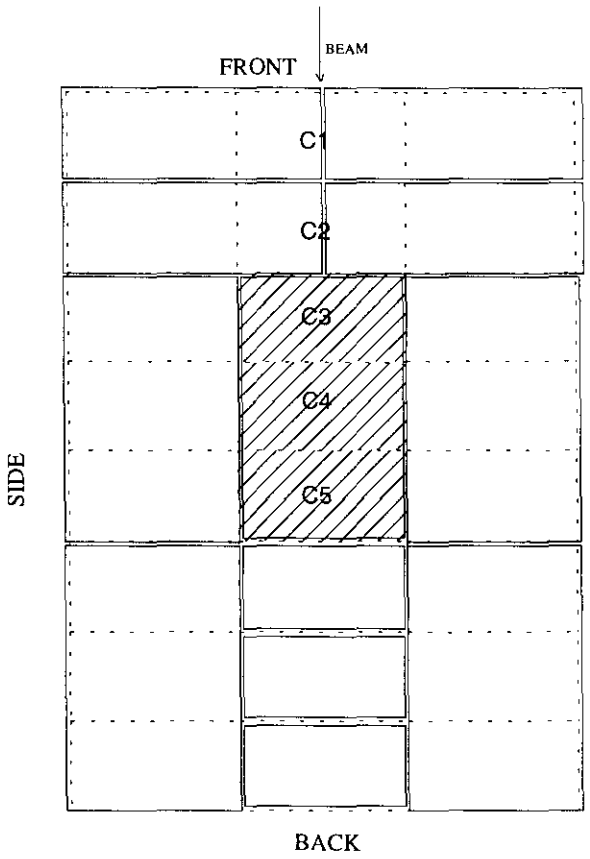

Fig. 2 Schematic view of the top of the dump showing the measurement grid. The positions are labelled C2 to C5 for consistency with results reported previously [7, 8].

experimental results (Table 2). The simulations were performed for protons only. In particular, a concrete wall placed at 3 m from the dump side was considered together with the floor. In the same simulation the air was also taken into account up to 20 m above the dump to include the skyshine effect. A further simulation was carried out by reducing the thickness of the scoring cells to 20 cm at position C3-C5. The influence of openings in between adjacent blocks was then investigated by considering a 2 cm aperture between positions C2 and C3 penetrating down to the iron core. The resulting values of ambient dose equivalent are listed in Table 1.

Table 2. Ambient dose equivalent of secondary neutrons around the dump produced by a 250 GeV/c proton/pion beam and by a lead ion beam at 158 GeV/c per nucleon. The exposure location is C4 (Fig. 2). Counting uncertainties are also listed.

	Ambient dose equivalent per primary particle (Sv)	
Detector	Proton/pion beam	Lead ion beam
LINUS	$(4.16\pm0.53)\times10^{-16}$	$(5.83\pm0.10)\times10^{-14}$
Studsvik	$(1.85\pm0.24)\times10^{-16}$	$(2.60\pm0.07)\times10^{-14}$

The following conclusions can be drawn:

1. the ambient dose equivalent due to secondary neutrons in the case of a primary pion beam is slightly lower than for protons. The inelastic cross section for protons at high energies are larger than those for positive pions of about a factor 1.6 [10]. This scaling factor can explain roughly

the lower values for pions, but the ratios of the results for the different beams in the various positions obviously also depend on neutron transport in the dump materials;

2. the influence of air and of the wall at 3 m from the side of the dump is negligible;
3. the thickness of the scoring cells on the dump top has little influence, showing that neutrons are mostly directed perpendicularly to the surface of the concrete blocks;
4. as expected, the openings in between adjacent blocks have a non negligible influence locally. The ambient dose equivalent in C2 increases by a factor 1.3, but in C3, which is at a higher level from the dump top (i.e. on the concrete step, Fig. 1) the effect is almost negligible. The discrepancy with measurements (Table 2) should be attributed to other slits and openings which were observed in the real structure, but which cannot be correctly modelled in the simulation.

The parallelepiped geometry turned out to be inadequate for calculating the neutron spectral fluence at the various positions, because most of the uncertainties in the considered 172 energy bins were too large (above 15-20%), with ten independent simulations with 5,000 primary particles for a global CPU time in the range 480-720 hours on a Digital Alpha Workstation. Therefore the spectral fluences calculated with the cylindrical approximation described in Section 2 were used as a guess for unfolding the experimental data. Fig. 3 shows the neutron spectral fluence on the lateral surface of the cylindrical dump upstream, i.e. close to the front surface, and downstream, i.e. close to the rear surface. The spectra in the intermediate positions have a similar shape and intermediate absolute values.

The lethargy spectra shown in Fig. 3 have a quasi-constant behaviour for energies below about 100 keV, characteristic of neutron slowing-down. A broad peak can be observed at a few MeV, representative of evaporation neutrons following the intranuclear cascade. A second, more distinguishable peak is present at about 100 MeV. This spectral shape is similar to that found outside a 80 cm concrete shield of the CERN-EC high-energy reference field facility [11, 12].

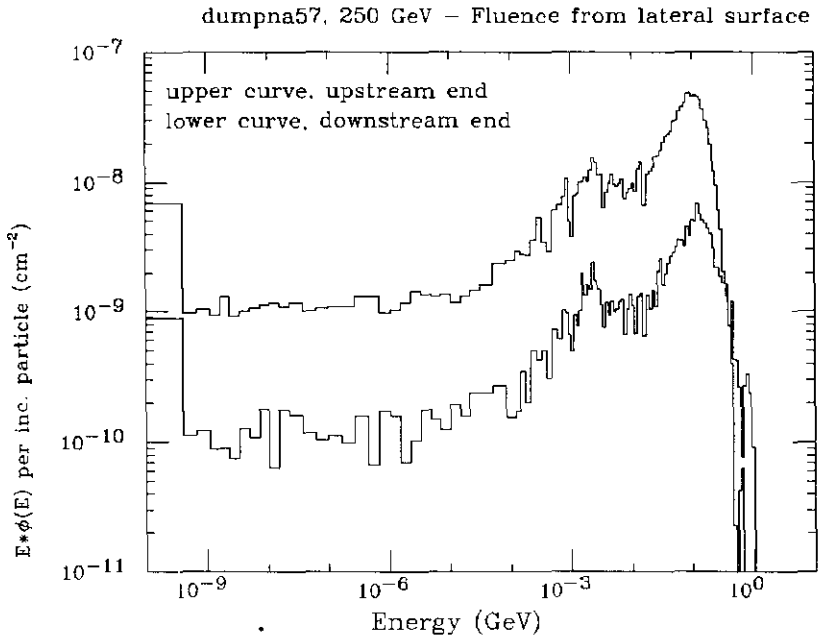

Fig. 3 Neutron spectral fluence on the lateral surface of the cylindrical dump used in the simulations.

4. Experimental

Measurements of the neutron ambient dose equivalent and of the neutron spectral fluence were performed on the top of the dump using different types of rem counters and a set of Bonner spheres, with both primary beams of 250 GeV/c protons/pions and lead ions of 158 GeV/c per nucleon. Other detectors were used for the measurements with the 250 GeV/c beam, namely a tissue equivalent proportional counter, a set of superheated drop detectors and other types of rem counters. These measurements are discussed elsewhere [7]; it should only be mentioned that the results obtained with the various instruments were in good agreement.

One of the Andersson-Braun rem counters was a commercial unit of conventional design, namely a Studsvik type 2202. The other was a spherical version of the LINUS rem counter [13-16], which is characterised by a modified moderator to extend its response to several hundreds MeV. Two LINUS detectors with a slightly different sensitivity were used and the results agreed within the experimental uncertainties.

Neutron spectrometry was performed with a Bonner sphere system. The spectrometer used a ^{3}He proportional counter, coupled with a set of six moderators: five polyethylene spheres (diameter 81 mm, 108 mm, 133 mm, 178 mm and 233 mm) and a spherical LINUS (diameter 236 mm) of the same type mentioned above. The sphere with diameter 81 mm was also exposed with a cadmium cover. The response functions of the six detectors are given in ref. [16]. The response of LINUS above 10 MeV compensates for the decreased sensitivity in the other measuring channels.

The proton/pion beam intensity was monitored with an air-filled ionisation chamber at atmospheric pressure, placed in the beam approximately 20 m upstream of the dump. This chamber could not be used with lead ions, because its response to these particles is not known. Therefore, one of the detectors used normally by one of the experiments was employed to monitor the lead ion beam, i.e. a Cherenkov quartz detector counting pulses from individual particles, installed about 10 m upstream of the dump.

The spectrometric measurements were performed at position C4 only (Fig. 2). It should be underlined that the region identified by positions C3-C5 is not too far from the cylindrical approximation used in the Monte Carlo calculation of the neutron spectral fluence. During the lead ion run, measurements were also performed on the dump lateral surface at a position corresponding to C4, where the shielding thickness is the same. The results agreed with those on the top within the statistical uncertainties.

The values of ambient dose equivalent measured with the two types of rem counters are given in Table 2. As expected, the dose equivalent measured by the conventional unit is lower by a factor of 2 with respect to that measured by the LINUS. This behaviour is easily explained by the high energy component of the energy spectrum (Fig. 3) and by the sharp decrease of the response function of the conventional rem counter above about 15 MeV.

5. Neutron spectrometry

The unfolding of the data acquired with the set of Bonner spheres was carried out by using a code largely based on the theories currently applied in the field of flux adjustment [17]. At each step, the code aims at reducing the χ^2–value arising from the experimental data, while limiting the modifications of the group fluxes with respect to the values of the previous iteration. In order to avoid negative values of the N group fluxes, their logarithm is evaluated instead. As initial guess for the unfolding of both the proton and lead ion data, the output of the FLUKA code, normalised to the sum of the experimental data, was used; the number of iterations is fixed according to the accepted χ^2–value. The procedure introduces some approximations and thus several iterations are required to reach the convergence, finely adjusting at each step the previous distribution.

As far the accuracy of the results is concerned, one can first notice that the experimental data of the Bonner spheres are always reproduced with a precision better than 5%, and in some case better than 1%. In this case, the presence of other types of uncertainties (e.g. due to calibration) cannot be

ignored, thus leading to larger global uncertainties. As for the FLUKA simulations, they are characterised by strongly varying statistical uncertainties, from a few percent in the region up to 1 MeV to much larger values in the high-energy region, due to the varying number of neutrons in the different energy bins. Consequently, the reconstructed spectra are less accurate in the high-energy region, also because of the very low response functions of the detectors, with the exception of the LINUS. Moreover, it was verified that experimental alterations of the input geometry lead to modifications in the medium-high energy region of the simulated spectra, so that also the statistical uncertainties provided by the code should be considered only as a rough indication. In addition, the use of the FLUKA results as a guess for the case of lead ions is purely tentative, and the total accuracy is even lower.

As a matter of convenience, due to the difficulty to carry out a quantitative sensitivity analysis, the number of iterations was fixed at 50, to reach a χ^2–value consistent with global data uncertainties in the range 3-6%. The uncertainties in the output group fluxes are thus largely undetermined, particularly above a few tens of MeV, where the reconstructed spectra only signal the presence of fluence, with a large statistical uncertainty in each energy group.

The results of the unfolding are shown in Fig. 4 for the proton and the lead ion beams, together with the guess resulting from the FLUKA simulations for protons. Fig. 5 shows the counts per beam particle for each Bonner detector (the sphere diameter is on the x-axis) and the LINUS.

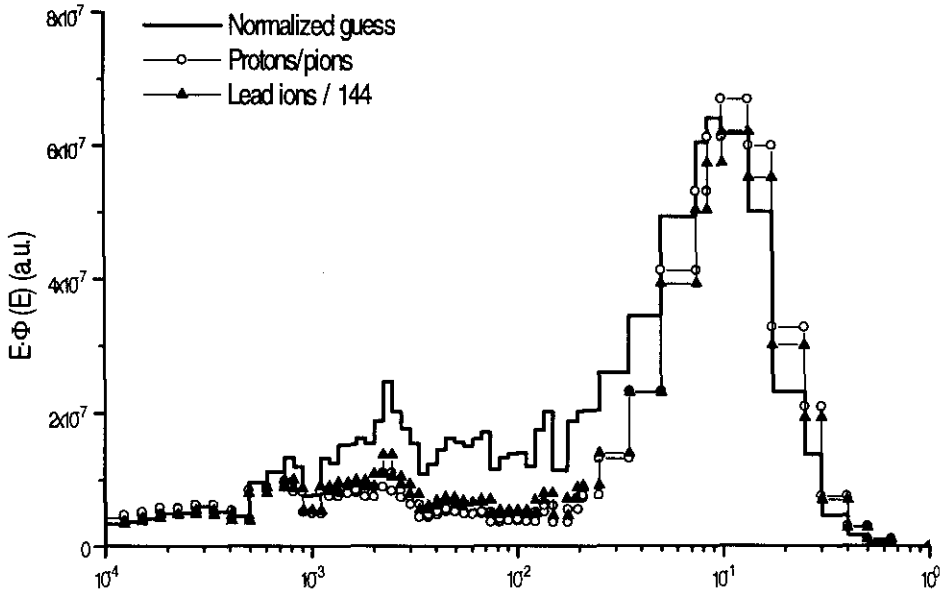

Fig. 4 Neutron spectral fluence resulting from the unfolding procedure for the proton/pion and the lead ion beams. The initial guess, calculated with the FLUKA code for the former case, is also shown. The data for lead ions are scaled to a factor of 144 (see text).

The counts reconstructed with the unfolding procedure are also plotted; they are in satisfactory agreement with the experimental ones. The solid curve shows the counts per primary particle calculated for the guess curve from which the iterative procedure starts.

6. Discussion

The counts per beam particle (Fig. 5) of the spectrometry detectors show the same behaviour for the proton/pion and the lead ion beams. The absolute values for the latter are larger, on average,

by a factor of 140. These results indicate that the secondary neutron spectra generated by the different primary beams have a similar shape even if the absolute yield is obviously different, as can be observed in the unfolded spectral fluences shown in Fig. 4. It should be pointed out that the shapes of the spectral fluences will nearly be the same if the same guess is chosen for unfolding the data for the proton/pion and the lead ion beams, as the ratio of the counts of the Bonner detectors is nearly constant.

The results of the neutron spectrometry and of the rem counter measurements indicate that the neutron component around the dump scales with the mass number of the projectile. Multiplying the results in Table 2 for the proton/pion beam by the lead ion mass (A=208), one obtains 8.6×10^{-14} and 3.8×10^{-14} Sv per primary particle for the LINUS and the Studsvik rem counters, respectively. For proton energies E_p above a few GeV the source term for lateral shielding and thick targets is independent of target material and scales with $E_p^{0.8}$ [1, 2]. The above figures have thus to be scaled by a factor accounting for the different beam energies:

$$(E_p/E_{Pb})^{0.8} = 1.44 \qquad (1)$$

where E_p and E_{Pb} are the energies per nucleon of the proton/pion and of the lead ion beams, respectively. This scales the values for the LINUS and the Studsvik rem counters to 6.0×10^{-14} and 2.7×10^{-14} Sv per primary particle, in remarkable agreement with the experimental values measured with lead ions and given in Table 2. The validity of this approach is confirmed by observing that when normalising the ion mass number A by the factor given by expression (1) one obtains 208/1.44=144, in perfect agreement with the factor 140 determined from the spectrometric measurements for the ratio of the absolute fluences. The neutron spectral fluence for lead ions in Fig. 4 has been scaled according to this factor.

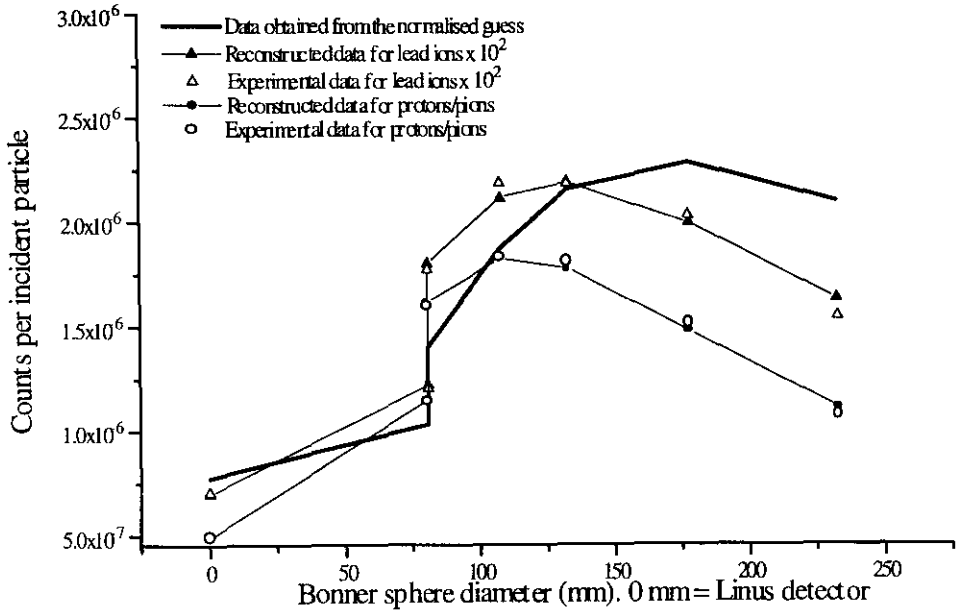

Fig. 5 Counts per primary particle as a function of detector diameter (the five Bonner spheres and the LINUS). The counts resulting from the unfolding procedure are also shown. The LINUS counts are placed at x=0. The data acquired with a cadmium cover are also plotted for the 81 mm sphere.

7. Conclusions

It has been shown that the spectral fluence of the secondary neutrons outside a thick shield is similar for light (protons) and heavy (lead) ions stopped in a thick target. It has also been shown that the approach of considering a high energy lead ion as a bunch of free protons is sufficiently accurate for the purpose of evaluating the ambient dose equivalent of secondary neutrons outside thick shielding. The neutron yield for hadrons dumped in a thick target can be assumed not only as energy dependent according to expression (1) but also linearly scaling with the mass number of the projectile. It should be underlined that this does not hold at energies below a few GeV, where the energy of the system (i.e., the energy of the individual nucleons) is of the same order of the rest mass of its constituents. Although one can expect that this assumption is valid for any projectile, it would be interesting to confirm it by measurements with another ion species. Whilst in a thick target the development of the hadronic cascade results in a variation of the neutron yield with energy as given above, with a thin target the high energy cross-sections vary much slower and are roughly equal to the geometrical value [18]. An experimental investigation of the neutron yield from high energy lead ions on a thin lead target is presently in progress.

Acknowledgements

The authors wish to thank F. Antinori, V. Manzari and F. Piuz for providing the beam monitoring during the lead ion run and for allowing us to install our monitoring equipment for the proton run.

References

[1] R.H. Thomas and G.R. Stevenson, Radiological safety aspects of the operation of proton accelerators, IAEA Technical Report Series No. 283, IAEA, Vienna (1988).

[2] A. Fassò, K. Goebel, M. Höfert, J. Ranft and G.R. Stevenson, Shielding against high energy radiation, Landolt-Börnstein, Vol. 11, H. Schopper, Ed., Springer-Verlag (1990), p. 126.

[3] A. Fassò, A. Ferrari, J. Ranft, P.R. Sala, G.R. Stevenson and J.M. Zazula, New developments in FLUKA modelling of hadronic and EM interactions, Proc. Third Workshop on Simulating Accelerator Radiation Environments (SARE3), KEK, Tsukuba, Japan, Ed. H. Hirayama, KEK Proceedings 97-5, p. 32 (1997).

[4] A. Ferrari, T. Rancati and P.R. Sala, Fluka applications in high-energy problems: from LHC to ICARUS and atmospheric showers, Proc. Third Workshop on Simulating Accelerator Radiation Environments (SARE3), KEK, Tsukuba, Japan, Ed. H. Hirayama, KEK Proceedings 97-5, p. 165 (1997).

[5] R.E. Prael and H. Lichtenstein, User guide to LCS: The LAHET Code System, LA-UR-89-3014, Los Alamos National Laboratory, Los Alamos, New Mexico (1989).

[6] N.V. Mokhov, S.I. Striganov, A. Van Ginneken, S.G. Mashnik, A.J. Sierk and J. Ranft, MARS code developments, Proc. of the Fourth Workshop on Simulating Accelerator Radiation Environments (SARE4), Knoxville (TN, USA), 14-16 September 1998, Ed. T. Gabriel, ORNL, p. 87 (1998).

[7] S. Agosteo, C. Birattari, A. Foglio Para, M. Silari and L. Ulrici, Beam dumps for high-energy hadrons: from design to reality, Proc. of the Fourth Workshop on Simulating Accelerator Radiation Environments (SARE4), T.A. Gabriel, Ed., Knoxville, Tennessee, September 14-16 1998, Publisher: Oak Ridge National Laboratory, p. 313 (1998).

[8] S. Agosteo, C. Birattari, A. Foglio Para, M. Silari and L. Ulrici, FLUKA simulations and measurements for a dump for a 250 GeV/c hadron beam, Mathematics and Computers in Simulation, in press.

[9] A. Ferrari and M. Pelliccioni, Fluence to dose equivalent conversion data and effective quality factors for high energy neutrons, Radiat. Prot. Dosim. 76 (1998) 215.

[10] Particle data group, Review of particle physics, Eur. Phys. J. C 3 (1998) 1.

[11] M. Höfert and G.R. Stevenson, The CERN-CEC high-energy reference field facility, Proc. the 8th International Conference on Radiation Shielding, Arlington, Texas, 24-28 April 1994, American Nuclear Society, p. 635 (1994).

[12] C. Birattari, A. Ferrari, M. Höfert, T. Otto, T. Rancati and M. Silari, Recent results at the CERN-EC high energy reference field facility, Proc. of the Third Specialists' Meeting on Shielding Aspects of Accelerators, Targets and Irradiation Facilities (SATIF3), Sendai (Japan), 12-13 May 1997, NEA/OECD, p. 219 (1998).

[13] C. Birattari, A. Ferrari, C. Nuccetelli, M. Pelliccioni and M. Silari, An extended range neutron rem counter, Nucl. Instrum. Meth. A 297 (1990) 250.

[14] C. Birattari, A. Esposito, A. Ferrari, M. Pelliccioni and M. Silari, A neutron survey-meter with sensitivity extended up to 400 MeV, Radiat. Prot. Dosim. 44 (1992) 193.

[15] C. Birattari, A. Esposito, A. Ferrari, M. Pelliccioni and M. Silari, Calibration of the neutron rem counter LINUS in the energy range from thermal to 19 MeV, Nucl. Instrum. Meth. A 324 (1993) 232.

[16] C. Birattari, A. Esposito, A. Ferrari, M. Pelliccioni, T. Rancati and M. Silari, The extended range neutron rem counter LINUS: overview and latest developments, Radiat. Prot. Dosim. 76 (1998) 135.

[17] M. Matzke, Unfolding of pulse height spectra: the HEPRO Program system. Braunschweig, Germany, PTB, Bericht 19 (1994).

[18] D.H. Perkins, Introduction to high energy physics, Addison-Wesley (1987), p. 134.